SAND96-1472C

# An Examination of Sandia's Phenomenological Computer Codes and the Use of Intelligent Searching in Risk Assessments*

CONF-960647--11

Allan S. Benjamin
Sandia National Laboratories
Albuquerque, New Mexico, USA

RECEIVED
JUL 02 1996
OSTI

**Abstract**

Because many of the phenomenologically based codes used to support risk assessments require long execution times, it is important to have a rationally based means for optimizing the choice of parameter values that are input to the code calculations. For this reason, we have developed a method for intelligently searching the space of parameter values to deduce, with as few computations as possible, the values that are most likely to lead to high risk. We have applied the method to a problem involving electrical initiation of an explosive due to the response of the system to fires. We have shown that our method can locate potential risk vulnerabilities with far fewer time-consuming physical response computations than would be necessary using standard sampling approaches.

## 1. Introduction

Sandia National Laboratories performs probabilistic risk and safety assessments for a variety of applications, including nuclear reactors, defense nuclear facilities, nuclear weapons, aerospace systems, telecommunication systems, transportation of hazardous materials, and storage of hazardous wastes. For these applications, Sandia has developed a variety of computer programs that perform various functions needed in a probabilistic risk assessment (PRA). They may be divided into two general categories: (1) system-based codes, such as those used for accident sequence evaluation and risk integration, and (2) phenomenologically based codes, such as those used for analysis of physical response, radionuclide transport, and health consequences. Whereas the system codes are usually quite fast-running, the complexities of the physical processes occurring during accident scenarios make it necessary to utilize fairly detailed, and therefore computer time-intensive, phenomenological codes.

Table I presents a summary of some of the principal phenomenological codes that have been developed at Sandia for various risk applications, and provides an estimate of the central processor unit (CPU) time required to estimate each code on its usual platform. It is clear that for some of these codes, using today's computers, it would not be practical to run more than a few tens of calculations for a given risk assessment. While tomorrow's computers will undoubtedly be faster than today's, the tendency in the future will be to increase the level of detail of the models in order to improve accuracy, fidelity, and predictive capability rather than to maintain the current level of detail and enjoy the savings in computer time. Thus, risk assessments will continue to be subject to the limitations of computer processing times.

Many of the more recent Level 3 risk assessments, starting most notably with NUREG-1150 [1], have attempted not only to characterize the risk emanating from a broad range of accident scenarios, but also to characterize the uncertainties in the risk associated with our imprecise or incomplete knowledge of material properties and physical phenomena. Standard Monte Carlo or Latin hypercube sampling processes [2] generate thousands, if not hundreds of thousands, of variations of parameters that are input to the phenomenological codes. Ideally, one would want to run the codes for each variation of parameters, but this would be impossible. The alternative is to have a reliable and yet very rapid means for estimating the response of the system over wide parameter ranges, and some of the codes in Table I are indeed formulated for this purpose. These less detailed, faster-running codes, however, must be calibrated to results from the more detailed codes.

Given that we must work with a limited number of detailed code calculations, there is a strong need for a rational means for optimizing the choice of parameter values that are input to the code calculations. Toward that end, we

* This work was supported by the United States Department of Energy under Contract DE-AC04-94AL85000.

Table I. Comparison of Some of Sandia's Phenomenological Computer Codes for Risk Applications

| Code Name | Ref. | Risk Application | Function | Typical CPU[a] |
|---|---|---|---|---|
| MELCOR | [3] | Nuclear Reactors | Progression of core degradation and containment response for severe accidents | 5-10 Hours/ Intel Pentium PC |
| MACCS | [4] | Nuclear Reactors | Dispersion and transport of radionuclides to environment and subsequent health effects | 2-4 Minutes[b] Intel Pentium PC |
| BRAGFLO | [5] | Radioactive Waste Storage | Multiphase flow of gas and brine through a porous reservoir | 3-6 Hours/ Digital VAX-α |
| SECO-FLOW | [6] | Radioactive Waste Storage | 2-D, single phase, Darcy flow for ground-water transport | 5-10 Minutes Digital VAX-α |
| SECO-TRANSPORT | [6] | Radioactive Waste Storage | Fluid flow and transport of radionuclides in fractured porous media | 3-6 Hours Digital VAX-α |
| TEMPRA | [7] | Nuclear Weapons | System thermal responses to timewise and spatially dependent fires | 20-40 Minutes Sun SPARC-20 |
| STRESS | [8] | Nuclear Weapons | System structural responses to impacts and punctures | 40-80 Minutes Sun SPARC-20 |
| MELTER | [9] | Transportation of Nuclear Materials | Approximate thermal responses to fires affecting cargoes in safe-secure trailers | 1-2 Seconds Sun SPARC-20 |
| ERAD | [10] | Transportation of Nuclear Materials | Turbulent atmospheric transport and diffusion following explosive releases | 20-40 Seconds Sun SPARC-20 |
| RADTRAN | [11] | Transportation of Nuclear Materials | Dispersion and public health consequences from ground transportation accidents | 20-40 Seconds[c] Sun SPARC-20 |

a: Per accident scenario or source term
b: Includes weather variations for one site
c: Includes location and demographic variations for one weather condition

have been investigating new methods for intelligently searching the parameter space, using both detailed and simplified models, to deduce the parameter combinations of most interest for the risk assessment. This paper describes one of our methods that has shown particular promise.

## 2. Use of Intelligent Searching in Risk Assessments

In the interest of clarity and precision, we will present our method in the context of a particular type of risk assessment. The concepts, however, should be applicable to a wide range of problems that involve phenomenological analyses of complex systems.

### 2.1 Example Problem

Suppose we have a system composed of $N$ electrical components that are connected at one end to an electrical source, such as a battery, and at the other end to a potential source of risk, such as an explosive. In normal circumstances, the battery and the explosive are separated from each other by a set of open switches and energy-transforming devices.

Suppose further that these components are encased in an insulating foam and placed in a container (see Fig. 1a), and that the container is exposed to a fire. Over a period of time, all the components will heat up. If the battery fluid boils, the battery will discharge electrical energy. If a switch reaches its melting temperature, it will close due to the formation of conductive bridges. If an energy-transforming device reaches its melting temperature, it will no longer be able to transform and pass electrical energy. If the explosive reaches its burning temperature, it will burn benignly rather than ignite.

In considering all the possible changes of state that can occur as a result of a fire, some are propagating in nature and some are terminating. The propagating events are the boiling of the battery fluid and the melting of the switches. The terminating events are the melting of the transforming devices and the burning of the explosive. In order for the explosive to ignite, all of the propagating events must occur before any of the terminating events. Thus, the switches must all begin to melt and the battery fluid must boil before any of the transforming devices begin to melt and before the explosive begins to burn.

Using a thermal analysis code, we determine that for the complete range of credible fire temperatures, there is no uniformly engulfing fire that can cause events to occur in the sequence necessary to create an ignition. Fig. 1b, which corresponds to a calculation for a real system similar in form to Fig. 1a, shows that both transforming devices reach their melting temperatures and the explosive reaches its burning temperature before any of the three switches reaches its melting temperature.

It may be possible for this system to experience an ignition, but we cannot know a priori under what conditions such an ignition might occur or how likely it is to occur without varying the parameters that describe the fire, the way that it is oriented toward the system, and the properties of the materials involved. To minimize the number of thermal analysis code runs to be performed, we must intelligently search the parameter space.

## 2.2 Synopsis of the Method

In assessments of the potential for an undesired outcome in an electrical system such as Fig. 1a, we define a quantity called "closeness to occurrence." For thermal environments, we define closeness in terms of races between components. The closeness of a race between a propagating event $A$ and a terminating event $B$ is expressed mathematically as follows:

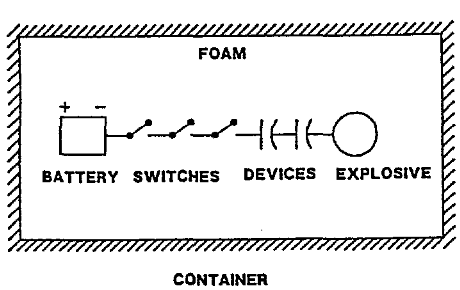


Figure 1a. Schematic of electrically initiated explosive system.

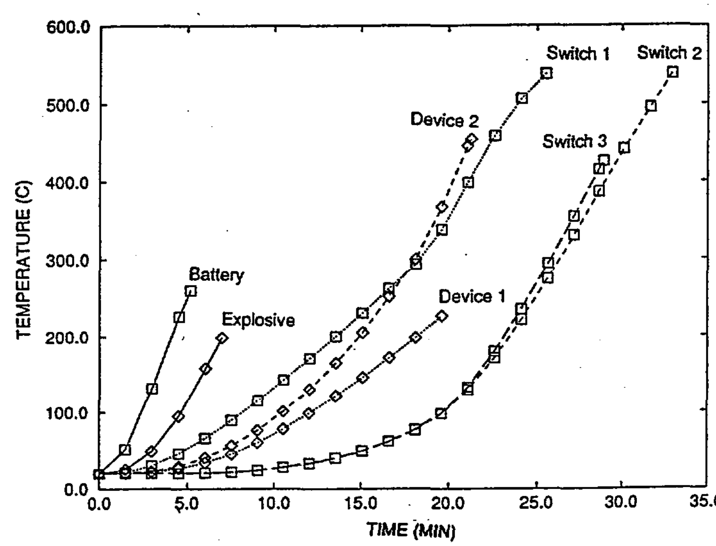


Figure 1b. Component temperatures versus time for an engulfing 1093 °C fire. Each curve is terminated at the point where phase change or reaction occurs.

$$K_{A,B} = \frac{T_{pk,A}(t_{fl,B}) - T_{in}}{T_{fl,A} - T_{in}} \tag{1}$$

where $T_{pk,A}(t)$ is the peak temperature achieved by Component $A$ up to time $t$; $T_{fl,A}$ is the failure temperature for Component $A$; $t_{fl,B}$ is the failure time for Component $B$ or the final time in the computation, whichever comes first; and $T_{in}$ is the initial temperature in the system. The race between $A$ and $B$ is lost if and only if $K_{A,B} \geq 1$. A vulnerability occurs when the race between $A$ and $B$ is part of the definition of a pathway leading to the undesired outcome. In principle, the term "pathway" as used here is synonymous with the PRA term "cut set," if one visualizes a fault tree in which the top event is the ignition of the explosive. In simple mathematical terms, the overall closeness to occurrence for a cut set $Z$ may be represented as follows:

$$K_Z = \min_{A,B \in Z} (K_{A,B}) \tag{2}$$

where $A,B \in Z$ denotes that $A$ and $B$ are both members of $Z$.

With this definition in hand, we may summarize the principal steps in the intelligent searching process for the problem under consideration. The procedure, which is outlined in Fig. 2, is incorporated into our computer code called SEARCH:

1. In the first iteration, a coarse hypercube of the input parameter space is set up and a thermal response computation is made at each "corner" of the hypercube (see Fig. 2a).
2. To account for some of the known nonlinearities, the temperature responses are divided by the fire temperature and the time scales are multiplied by the fourth power of the fire temperature. This normalization of the primitive variables enables us to incorporate our preknowledge of the first-order response characteristics of the system. For example, the time for a component to achieve a certain level of temperature is inversely proportional to the radiative heat flux from the fire to the system as a whole, and the latter is proportional to the fourth power of the fire temperature over the range of temperatures of interest in the risk assessment.
3. Using the results from Steps 1 and 2, an estimator in the form of a response surface is developed for each of the following measures of response: (a) the normalized peak temperature achieved by each component during the accident scenario, and (b) the times to reach various fractions of the peak temperature (see Fig. 2b). Taken together, these responses approximate the total temperature-time history for the component. The response equations can be viewed as truncated Taylor series and the coefficients in the response equations as the first-order partial derivatives of the responses with respect to each of the input variables together with all the associated cross derivatives (see Fig. 2b).
4. A very finely divided hypercube of the same parameter space is set up (see Fig. 2c), and the component responses are estimated for each intersection point using the response surfaces derived in Step 3. For each point, the estimations of component physical response are used to determine race closenesses using Equation (1), and the race closenesses are used to estimate the overall closeness to occurrence for each cut set using Equation (2).
5. The results from Step 4 are then binned according to user prescription (see Fig. 2d). Each bin represents a subset of the total parameter space, defined so as to encompass physically similar situations. For each bin, the boundaries of any "islands of vulnerability" are determined by inspection of the estimates obtained in Step 4, and the location of the center of the island is similarly estimated. The term "island" is used to represent a region of the parameter space for which the overall closeness to occurrence is greater than or equal to 1.0.
6. The results from Step 5 are evaluated to determine which potential islands of vulnerability are most credible and which parameters are most important for that particular vulnerability. (The importance of a parameter is defined here as the relative sensitivity of the closeness to occurrence to variations in that parameter.) Based on these findings, a number of estimated island centers are selected for further analysis (see Fig. 2d).
7. For each island center selected in Step 6, a subspace is defined in which the less important parameters are held at fixed values while the more important ones vary over their defined ranges. The subspace is then partitioned so that the estimated island center becomes the common point of generation for the partitions (see Fig. 2d).

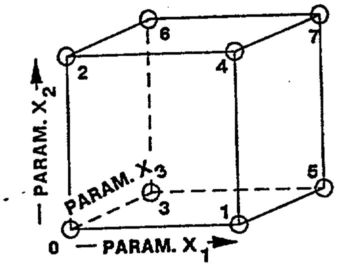


Fig. 2a. Schematic of parameter hypercube and initial thermal response computations (example for 3 input parameters). Circles denote physical response runs.

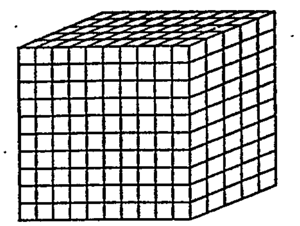

Fig. 2c. Schematic of estimator sampling matrix (example for 3 input parameters). Intersections denote sampling points.

Thermal Response

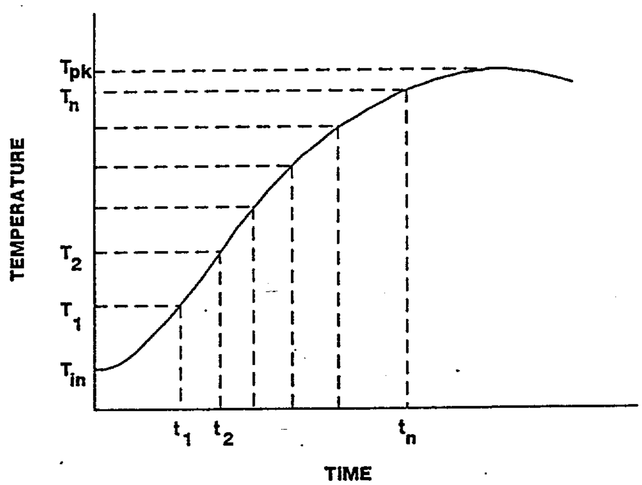


Response Parameters:

$$Y_1 = \frac{T_{pk} - T_{in}}{T_{fire} - T_{in}} \qquad Y_{i+1} = t_i \frac{T_{fire}^4 - T_{in}^4}{T_{in}^4} \quad (i = 1,2,\ldots,n)$$

Response Equation (Example for 3 Input Parameters)

$$Y_i = C_{0,i} + C_{1,i}\Delta X_1 + C_{2,i}\Delta X_2 + C_{3,i}\Delta X_3 + C_{4,i}\Delta X_1 \Delta X_2 + C_{5,i}\Delta X_1 \Delta X_3 + C_{6,i}\Delta X_2 \Delta X_3 + C_{7,i}\Delta X_1 \Delta X_2 \Delta X_3$$

Figure 2b. Schematic of component thermal response, response parameters, and response surface equation form.

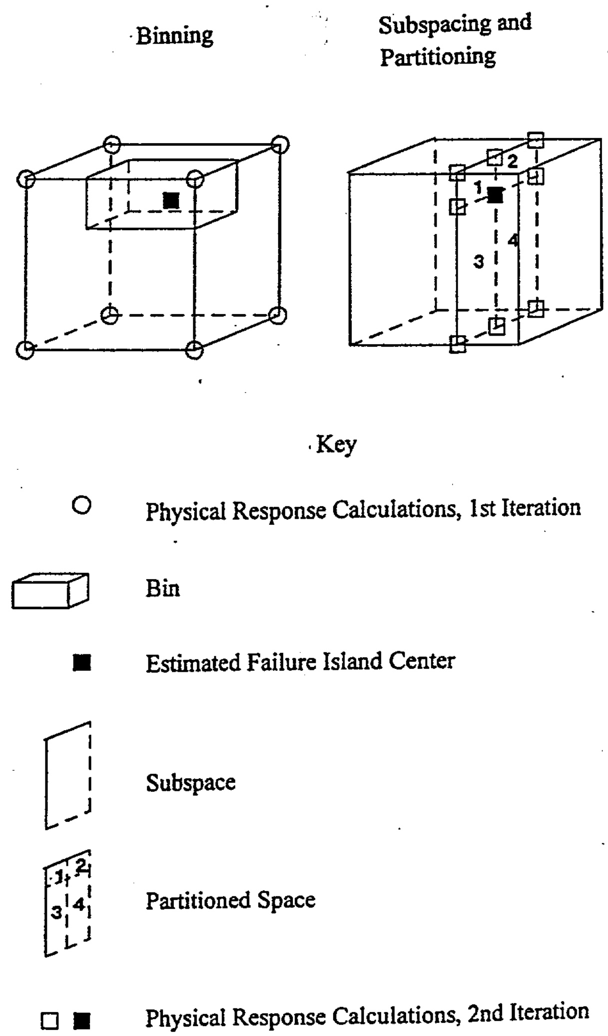


Figure 2d. Schematic of parameter binning, subspacing, and partitioning.

8. New thermal response computations are performed at corners of the partitions for which a physical response computation has not previously been performed. Based on these new computations, a new set of response surface equations is developed for each partition.

9. Steps 4 and 5 are repeated for each new partition, using the new response surface equations developed in Step 8. If the results from Step 6 are notably different from the previous iteration, the iterative process is repeated starting from Step 6.

## 2.3 Example Results

We applied the intelligent searching method described above to a detailed physical model based on Fig. 1a in order to investigate the convergence properties and computational efficiency of the method. The parameter space to be sampled included four input variables, which are summarized below:

1. Exposure Patterns: The container was assumed to be partially immersed in a sheltering medium. Portions on one side of the immersion plane were exposed to the fire, portions on the other side were protected from it. The plane could take various orientations with respect to the container.
2. Thermal model for the foam: Two models were sampled. (a) heat transfer through the foam governed by thermal radiation; and (b) heat transfer governed by thermal conduction.
3. Heat transfer coefficient for the immersing medium: Values could range from 0 (insulating medium) to 0.1 cal/cm$^2$-s-°C (convective liquid).
4. Fire temperature: Values could range from 550 °C to 2750 °C.

One of the exposure patterns is shown in Fig. 3a, and representative results for that pattern are shown in Fig. 3b. The latter figure depicts results for a cut through the parameter hypercube, in which the variation of the overall closeness to occurrence with fire temperature is shown with all other variables held constant.

In the first iteration, we performed 36 thermal response computations to cover the most significant corners of the parameter hypercube and to develop the response surface equations. None of these runs happened to fall within the cut of Fig. 3b. We then applied the resulting response equations at approximately 50,000 points in the hypercube to estimate the responses of the system to a wide spectrum of parameter variations. In subsequent iterations, we partitioned the temperature scale at the most significant local peaks and performed a few additional thermal response calculations as indicated in the figure.

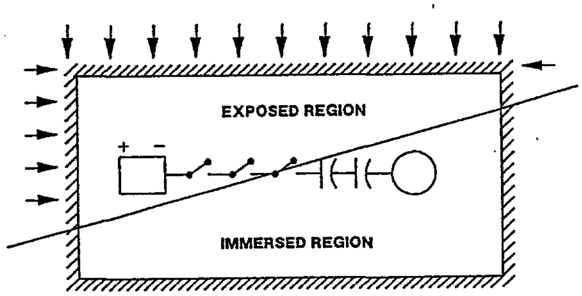


Figure 3a. Schematic of a fire exposure pattern.

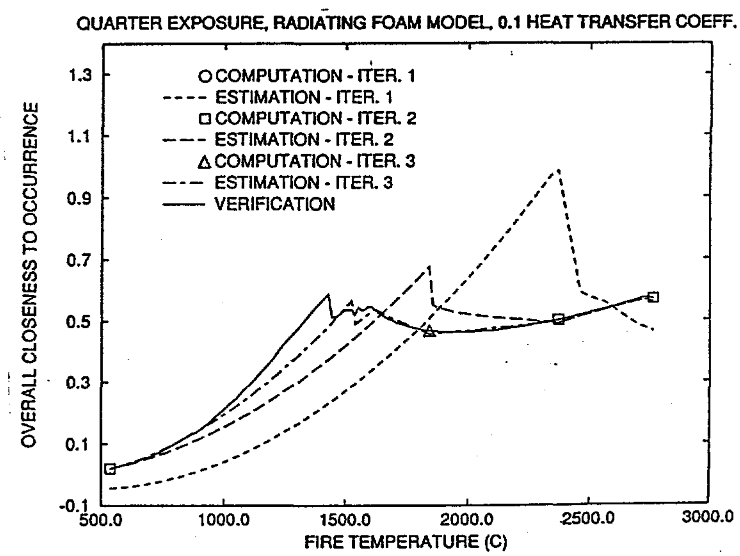


Figure 3b. Variation of overall closeness to occurrence with fire temperature, other conditions as indicated.

It may be seen that only three iterations were required for the method to converge quite closely to the correct location and peak value of the principal failure island of Fig. 3b. We verified that the code had converged to the correct values by performing an additional set of thermal response runs in order to obtain the solid curve in the figure.

From the results obtained so far, the intelligent searching process appears to be able to characterize the failure islands of the example problem quite accurately with approximately one-tenth as many physical response calculations as would be required by a random sampling process without the benefit of intelligent searching. The amount of CPU time required for the entire search, exclusive of the thermal response calculations, was only about 10 minutes on a Sun SPARC-10 workstation.

## 3. Conclusions

For the particular type of problem considered, the approach for intelligent searching described in this paper has the potential for locating vulnerabilities of very low probability and appears to require far fewer time-consuming computations for physical response determination than standard sampling methods. The results indicate, in addition, that the process should scale well with increasing size and complexity of a problem.

The specifics of the approach have to be tailored to the particular risk application being studied. In the future, we hope to investigate the utility of the method for a variety of risk applications.

## References


1. Reactor Risk Reference Document. NUREG-1150, U.S. Nuclear Regulatory Commission, Washington, DC, 1987.
2. Iman, R. L., and Shortencarier, M. J., "A FORTRAN 77 Program and Users Guide for the Generation of Latin Hypercube and Random Samples for Use with Computer Models," NUREG/CR-3624, SAND83-2365, Sandia National Laboratories, Albuquerque, NM, 1984.
3. Summers, R. M., et al. MELCOR Computer Code Manuals, Vol. 1, Primer and Users Guides, Version 1.8.3. NUREG/CR-6119, SAND93-2185, Sandia National Laboratories, Albuquerque, NM, 1995.
4. Chanin, D. I., et al. MELCOR Accident Consequence Code System (MACCS). NUREG/CR-4691, SAND86-1562, Sandia National Laboratories, Albuquerque, NM, 1990.
5. Helton, J. C., Anderson, D. R., Baker, B. L., et al. Effect of Alternative Conceptual Models in a Preliminary Performance Assessment for the Waste Isolation Pilot Plant. Nuclear Engineering and Design, 1995; 154:251-344.
6. Roach, P. J. The SECO Suite of Codes for Site Performance Assessment. Proceedings of 4th International Conference on High Level Radioactive Waste Management, American Nuclear Society, 1993.
7. Benjamin, A. S., Beraun, R., Brown, N. N., and Sherman, M. P. Evaluation of Conductive, Radiative, Chemical, and Convective Heat Transfer in Complex Systems Using a Fast-Running, Implicit, Lumped Capacitance Formulation. National Heat Transfer Conference. American Society of Mechanical Engineers. Portland, Oregon, 1995.
8. Benjamin, A. S., and Altman, B. S. Evaluation of Nonlinear Structural Responses Using a Fast-Running Spring-Mass Formulation. International Conference on Computational Engineering Science. Mauna Lani, Hawaii, 1995.
9. Larsen, M. E. MELTER: A Model of the Thermal Response of Cargos Transported in the Safe-Secure Trailer Subject to Fire Environments for Risk Assessment Applications. SAND93-0737, Sandia National Laboratories, Albuquerque, NM, 1994.
10. Boughton, B. A., and DeLaurentis, J. M. Description and Validation of ERAD: An Atmospheric Dispersion Model for High Explosive Detonations. SAND92-2069, Sandia National Laboratories, Albuquerque, NM, 1992.
11. Neuhauser, K. S., and Kanipe, F. L. RADTRAN 4.0, Volume 3, User Guide. SAND89-2370, Sandia National Laboratories, Albuquerque, NM, 1992.